

# Kinetics of uranium(VI) lability and solubility in aerobic soils

M. Izquierdo<sup>ab\*</sup>, S.D. Young<sup>a</sup>, E.H. Bailey<sup>a</sup>, N.M.J. Crout<sup>a</sup>, S. Lofts<sup>c</sup>, S.R. Chenery<sup>d</sup> and G. Shaw<sup>a</sup>

<sup>a</sup>School of Biosciences, University of Nottingham, Sutton Bonington Campus, Loughborough, LE12 5RD, United Kingdom

<sup>b</sup>Institute of Environmental Assessment and Water Research, 18-26 Jordi Girona, Barcelona 08034, Spain

<sup>c</sup>UK Centre for Ecology and Hydrology, Lancaster Environment Centre, Library Avenue, Bailrigg, Lancaster, LA1 4AP, United Kingdom

<sup>d</sup>British Geological Survey, Environmental Science Centre, Keyworth, Nottingham, NG12 5GG, United Kingdom

\*corresponding author: maria.izquierdo@idaea.csic.es Tel. +34934006146

## ABSTRACT

Uranium may pose a hazard to ecosystems and human health due to its chemotoxic and radiotoxic properties.

The long half-life of many U isotopes and their ability to migrate raise concerns over disposal of radioactive wastes. This work examines the long-term U bioavailability in aerobic soils following direct deposition or transport to the surface and addresses two questions: (i) to what extent do soil properties control the kinetics of U speciation changes in soils and (ii) over what experimental timescales must U reaction kinetics be measured to reliably predict long-term of impact in the terrestrial environment? Soil microcosms spiked with soluble uranyl were incubated for 1.7 years. Changes in U<sup>VI</sup> fractionation were periodically monitored by soil extractions and isotopic dilution techniques, shedding light on the binding strength of uranyl onto the solid phase. Uranyl sorption was rapid and strongly buffered by soil Fe oxides, but U<sup>VI</sup> remained reversibly held and geochemically reactive. The pool of uranyl species able to replenish the soil solution through several equilibrium reactions is substantially larger than might be anticipated from typical chemical extractions and remarkably similar across different soils despite contrasting soil properties. Modelled kinetic parameters indicate that labile U<sup>VI</sup> declines very slowly, suggesting that the processes and transformations transferring uranyl to an intractable sink progress at a slow rate regardless of soil characteristics. This is of relevance in the context of radioecological assessments, given that soil solution is the key reservoir for plant uptake.

**Keywords:** uranium, soil, humus, iron oxide, bioavailability, isotopic dilution

## 1. INTRODUCTION

Uranium is considered a potential hazard to ecosystems and human health due to its chemotoxic and radiotoxic properties (Alloway, 2012). Contamination is widespread (Gavrilescu et al., 2009); sources include nuclear weapons, nuclear reactor operations, nuclear accidents, waste disposal (Vandenhove et al., 2007a) and mining activities (Lottermoser et al., 2011). In reducing environments, tetravalent  $U^{IV}$  is typically present as insoluble uraninite  $U^{IV}O_2(s)$ , although numerous recent works have identified non-crystalline disordered  $U^{IV}$  phases in soils and sediments (Fuller et al. 2020 and references therein). Under oxidising conditions,  $U^{VI}$  as the uranyl cation ( $U^{VI}O_2^{2+}$ ) is the common species. Uranyl is relatively mobile (Cumberland et al., 2016) and is the major species responsible for U toxicity in aquatic organisms (Crawford et al., 2017). The presence of complexing ligands in groundwater may enhance U mobility. Thus, groundwater interactions with waste deposits influence safety assessment of radioactive waste repositories (Krupka et al., 1999; Um et al., 2010; Vandenhove et al., 2007a). The long half-life of many U isotopes (i.e.  $10^5 - 10^8$  yr) and their ability to migrate as complexed and free uranyl forms raise concerns over geological disposal of radioactive wastes.

Radioisotope solubility is often expressed as a solid-liquid distribution coefficient ( $K_d$ ); compilations exist for U (e.g. Crawford et al. 2017; Krupka et al., 1999; Sheppard et al., 2006, 2009). Values of  $K_d$  are typically obtained after 'spiking' soils (Krupka et al., 1999) and incubating these under suitable conditions. However, the resulting data are typically based on relatively short contact times ranging from hours (Manoj et al., 2019) to weeks (Vandenhove et al., 2007a) and, rarely, months (Elless and Lee, 1998). Such an approach is unlikely, therefore, to provide true 'equilibrium'  $K_d$  values. The large variation seen in compilations of U  $K_d$  values largely reflects a strong dependence on soil properties, especially pH (Sheppard et al., 2009). Echevarria et al. (2001) found a linear relationship between soil pH and U sorption, whilst soil texture and organic matter were not significant. However, Cumberland et al. (2016) and Fuller et al. (2020) demonstrated the relevance of U complexation with humic substances, which can influence U mobility and  $K_d$  values. Thus,  $K_d$  values are subject to uncertainties that may compromise disposal risk assessments if site-specific factors are not considered.

53 Numerous studies have attempted chemical fractionation of U using sequential extractions. Typically,  
54 the so-called 'exchangeable' and 'carbonate-bound' fractions are recognised as readily available (Rout et al.,  
55 2016). In a pot experiment, Vandenhove et al. (2014) found a relationship between U concentration in the  
56 exchangeable fraction of soils and in ryegrass. As a complement to chemical extractions, isotopic dilution  
57 assays have the potential to add new insights into time-dependent changes in U speciation. The technique  
58 consists on adding a known amount of an isotopic tracer to a soil suspension in equilibrium; the resulting  
59 change in isotopic ratios gives an indication of the isotopically exchangeable concentration, which provides a  
60 more mechanistically based estimate of the reactive pool (Young et al., 2005, 2006). Hamon et al. (2008) and  
61 Midwood (2007) provide descriptions of the principles of the technique. To date very little is known about U  
62 isotopic exchangeability in aerobic soils as the literature is limited to contaminated sediments (Bond et al.,  
63 2007; Kohler et al., 2004; Um et al., 2010). To our knowledge, changes in U isotopic exchangeability in aerobic  
64 soils, and the influence of soil properties, have not been addressed.

65 In this work we examined time-dependent changes in the lability and solubility of U in a wide range of  
66 soils, incubated under aerobic conditions for 1.7 yr following contamination. The study monitored changes in  
67 U fractionation, specifically the 'soluble', 'chemically exchangeable' and 'isotopically exchangeable' U  
68 fractions, thereby providing mechanistic insights into the kinetics of U adsorption and immobilisation in  
69 aerobic soils over time. Ultimately our main aim was to address two questions: (i) to what extent do soil  
70 properties control the kinetics of U speciation changes in aerobic soils and (ii) over what experimental  
71 timescales must U reaction kinetics be measured in order to make reliable long-term predictions of impact in  
72 the terrestrial environment?

## 73 **2. MATERIALS AND METHODS**

### 74 **2.1. *Soil sampling and characterisation***

75 Twenty topsoil samples (0–15 cm depth) with contrasting properties were collected from locations in  
76 the UK (Table 1) and sieved to <4 mm. A portion was oven dried (105°C) and ground for acid digestion. This

77 was undertaken in Savillex™ vials with concentrated, *Primar Plus*™ HF, HNO<sub>3</sub> and HClO<sub>4</sub> using a stepped heating  
78 program up to 160°C. Duplicate certified reference soils and sediments NIST SRM 2711a, NIST 1646a and IRMM  
79 BCR-167 and reagent blanks were also digested. Elemental recoveries were >80% for the majority of the  
80 certified elements.

81 Soil pH was measured in 0.01 M CaCl<sub>2</sub> suspensions (2.5 L kg<sup>-1</sup>). Organic C contents (OC) were  
82 determined using a FLASH EA1121 CNS analyser. Total free oxides (Fe<sub>FREE</sub>, Al<sub>FREE</sub> and Mn<sub>FREE</sub>) were extracted by  
83 shaking soil with Na-citrate and Na-dithionite for 24 h in a 20°C water bath (Olsen and Roscoe, 1982). Estimates  
84 of amorphous and poorly crystalline oxides (Fe<sub>AM</sub>, Al<sub>AM</sub> and Mn<sub>AM</sub>) were obtained following extraction in  
85 ammonium oxalate and oxalic acid, shaken in darkness for 2 h (Schwertmann, 1973). All filtered solutions (<0.2  
86 µm) were acidified to 2% HNO<sub>3</sub> before analysis.

## 87 **2.2. Soil microcosm incubation and soil extractions**

88 Portions of ~1.7 kg (dry soil basis) of partially air-dried soils were contaminated with 5000 µg U<sup>VI</sup>O<sub>2</sub><sup>2+</sup> per  
89 kg dry soil, using a Spex CertiPrep uranium standard solution (10000 µg mL<sup>-1</sup>) in 2.5% HNO<sub>3</sub> diluted 1-in-4. To  
90 this end, approximately 3.4 mL of the U spike were slowly added to each soil while the samples were  
91 mechanically stirred (c. 60 rpm) with the aid of a food mixer for 4 minutes to ensure uniform contamination.  
92 This represented a 2 – 7 fold increase in background U concentrations, which ranged between 700–5000 µg  
93 kg<sup>-1</sup>. The moisture contents were readjusted with ultrapure water during soil mixing. No attempt was made to  
94 achieve a pre-determined water content; rather, a friable but moist consistency was sought to aid soil mixing,  
95 which required different volumes of water to be added to individual soils. Each contaminated soil was  
96 distributed between three 1 L glass bottles (microcosms) with a hole in the lid to allow gas exchange and  
97 incubated in darkness at 10°C for 619 days. The microcosms were regularly hand shaken to aid aeration, and  
98 soluble Mn and Fe were monitored during periodic soil extractions as indicators of any redox changes. Further  
99 details on the experimental setup and microcosm sampling are reported in Izquierdo et al. (2019).

100 Changes in soluble U (U<sub>sol</sub>) were determined by sampling each microcosm and equilibrating the  
101 equivalent of 4.0 g dry soil with 20 mL 0.01 M KNO<sub>3</sub> for 16 h on an end-over-end shaker. The soil suspensions

102 were centrifuged (3000rpm, 20 min) and filtered through cellulose nitrate syringe filters (0.22 µm pore size).  
103 An aliquot was adjusted to 2% HNO<sub>3</sub> prior to analysis. The remaining solution was used for dissolved organic  
104 carbon (DOC) analysis.

105 Chemically exchangeable ( $U_{\text{exch}}$ ) and isotopically exchangeable ( $U_E$ ) fractions of U were simultaneously  
106 determined in the same solution extracts. At each sampling time, a portion equivalent to 2.0 g dry soil was  
107 equilibrated with 20 mL 1 M Mg(NO<sub>3</sub>)<sub>2</sub> containing the equivalent of 6 µg <sup>233</sup>UO<sub>2</sub><sup>2+</sup> and 6 µg <sup>236</sup>UO<sub>2</sub><sup>2+</sup> per kg dry  
108 soil. This was prepared from the Certified Reference Material IRMM-3636 with certified mass fractions of <sup>233</sup>U  
109 and <sup>236</sup>U of 50.135% and 49.832% respectively. The soil suspensions were shaken for 36 hours, centrifuged  
110 (3000rpm, 30 min) and filtered through 0.22 µm cellulose nitrate filters, and the supernatant was adjusted to  
111 2% HNO<sub>3</sub> prior to analysis.

112 The values reported in this work are the average of 3 replicated microcosms. The coefficients of  
113 variation were typically between 2 – 10% for the three different soils extractions, suggesting that the U<sup>VI</sup>O<sub>2</sub><sup>2+</sup>  
114 addition was evenly distributed during experimental soil mixing prior to incubation.

### 115 **2.3. Analyses of solutions and calculations**

116 The acid digests and soil extracts were analysed using ICP-MS (iCAP-Q; Thermo Fisher Scientific, Bremen,  
117 Germany) and Ir and Rh as internal standards. Dissolved inorganic carbon (DIC) and DOC were determined  
118 using a Shimadzu TOC-Vcp analyser.

119 The isotopic composition of the soil extracts was determined using ICP-MS with Ir as internal standard. Peak  
120 dwell times for <sup>233</sup>U, <sup>236</sup>U and <sup>238</sup>U were 0.5 s, with 450 quadrupole sweeps. The <sup>233</sup>U/<sup>236</sup>U spike was included  
121 every 12 samples to drift-correct for mass discrimination. The isotopically exchangeable U was estimated from  
122 Eq. 1 (Tye et al. 2002):

$$123 \quad U_E (\mu\text{g g}^{-1}) = {}^{238}\text{U}_{ss} \left( K_d^* + \frac{V_{ss}}{w_{\text{soil}}} \right) \quad (\text{Eq. 1})$$

124 where  $^{238}\text{U}_{ss}$  is the concentration of  $^{238}\text{U}$  in the solution phase of the soil suspension ( $\mu\text{g L}^{-1}$ ),  $V_{ss}$  is the volume  
125 of extractant (L),  $w_{\text{soil}}$  is the soil mass (kg) and  $K_d^*$  ( $\text{L kg}^{-1}$ ) is distribution coefficient of the enriched isotope, and  
126 therefore also the  $K_d$  of the isotopically exchangeable soil U (Eq. 2):

$$127 \quad K_d^* = \frac{{}^{23x}\text{U}I_{\text{adsorbed}}}{{}^{23x}\text{U}I_{ss}} \quad (\text{Eq. 2})$$

128 In Eq 2,  ${}^{23x}\text{U}I_{\text{adsorbed}}$  is calculated from the difference between the intensities (cps) of  $^{233}\text{U}$  and  $^{236}\text{U}$  in the spike  
129 and their intensities in the suspension solution phase;  ${}^{23x}\text{U}I_{ss}$  is the measured intensity of  $^{233}\text{U}$  or  $^{236}\text{U}$  in the  
130 solution phase of the soil suspension.

131 A standard soil-solution partition coefficient for the soil U was calculated (Eq 3):

$$132 \quad K_d (\text{L kg}^{-1}) = \frac{C_0 + C_{\text{spike}}}{U_{\text{sol}}} \quad (\text{Eq. 3})$$

133 Where  $C_0$  denotes the concentration of native U in soils ( $\mu\text{g kg}^{-1}$ ),  $C_{\text{spike}}$  is the U concentration added to soils  
134 ( $\mu\text{g kg}^{-1}$ ) and  $U_{\text{sol}}$  is the U concentration ( $\mu\text{g L}^{-1}$ ) in the 0.01 M  $\text{KNO}_3$  extracts.

135 In addition, the partitioning ( $K_d^L$ ,  $\text{L kg}^{-1}$ ) between adsorbed isotopically exchangeable U and the free  
136 uranyl ion in solution was also calculated (Eq. 4) (Mossa et al., 2020).

$$137 \quad K_d^L (\text{L kg}^{-1}) = \frac{U_E - U_{\text{sol}}}{(UO_2^{2+})_{\text{sol}}} \quad (\text{Eq. 4})$$

138 Where  $U_E$  is the concentration of isotopically exchangeable U in soils ( $\text{mol kg}^{-1}$ ),  $U_{\text{sol}}$  ( $\text{mol kg}^{-1}$ ) is the U  
139 concentration extracted with 0.01 M  $\text{KNO}_3$  and  $(UO_2^{2+})$  is the free ion activity ( $\text{mol L}^{-1}$ ) in the solution phase of  
140 the  $\text{KNO}_3$  extracts speciated using WHAM7.

141

## 142 **2.4. Geochemical speciation**

143 The geochemical speciation model WHAM7 (Lofts and Tipping, 2011) was used to estimate the speciation of  
144  $\text{U}^{\text{VI}}$  in the solution phase of soil suspensions equilibrated in 0.01 M  $\text{KNO}_3$ . The modelling approach assumes  
145 that all U is present as uranyl  $\text{U}^{\text{VI}}$  and simulates uranyl binding to dissolved organic matter and Fe oxide colloids  
146 in the solution phase (Lofts et al., 2015). Input data included soil pH, temperature (277K) and solution

147 concentrations of Na, Mg, Al, K, Ca, Fe, Mn and U. Colloidal (dissolved) fulvic acid (FA) was included, assuming  
148 that FA consists of 50% DOC and only 65% is active with respect to ion binding (Tye et al., 2004). The carbonate  
149 system was simulated from measured DIC. WHAM7 was used with an augmented database (Lofts et al., 2015).  
150 Two modelling scenarios were tested: (i) FA as the only colloidal phase present in the system; (ii) colloidal FA  
151 and sub-micron colloidal hydrous ferric oxides (HFO). This was addressed by allowing Fe<sup>III</sup> to precipitate as  
152 colloids with active surface chemistry in the simulation, using binding parameters from Lofts et al. (2015).

153 Fractionation of labile U across the whole soil-solution system was also attempted. The solid binding  
154 phases included (i) oxides, for which the two sets of estimates (Fe<sub>FREE</sub>, Al<sub>FREE</sub> and Mn<sub>FREE</sub>; Fe<sub>AM</sub>, Al<sub>AM</sub> and Mn<sub>AM</sub>)  
155 were tested in separate simulations; (ii) particulate humic acid (HA) estimated from OC assuming that 50%  
156 consists of active humic material (Buekers et al., 2008); (iii) geocolloidal species actively binding U in solution  
157 i.e. FA and HFO, as described above. We also assessed the use of WHAM7 to predict U<sub>sol</sub> concentrations from  
158 basic soil characteristics.

## 159 **2.5. Modelling U kinetics**

160 Time-dependent reductions in both U<sub>sol</sub> and U<sub>E</sub> concentrations were described using single rate exponential  
161 models with an 'offset' representing a persistently soluble or labile fraction, respectively (Eq. 5):

$$162 \quad U_x(t) = A \cdot e^{-tk} + B \quad (\text{Eq. 5})$$

163 where U<sub>x</sub>(t) is the concentration of soluble or labile U at any time t after initial contamination of the soils; A is  
164 the soluble or labile U (μg kg<sup>-1</sup>) after 4 days incubation subject to depletion; B is the U persistently remaining  
165 soluble or labile fraction; k is the first-order rate coefficient (t<sup>-1</sup>) representing the rate of depletion of A. The  
166 model was fitted to experimental data from each soil using Microsoft Excel® 'Solver'. The rate coefficients in  
167 Eq. 5 were used to estimate the times required to deplete by half the U<sub>sol</sub> or U<sub>E</sub> concentration measured after  
168 4 days (Eq. 6):

$$169 \quad T_{1/2} (\text{days}) = \frac{\ln(2)}{k} \quad (\text{Eq. 6})$$

### 170 3. RESULTS AND DISCUSSION

#### 171 3.1. Soil characterisation

172 The general properties of the studied soils are reported in Table 1. Organic C varied between 1.7 – 38.6%  
173 strongly reflecting different land uses. Soil pH ranged between 3.4 – 8.0, with the lowest values reported for  
174 a soil overlying pyrite-rich bedrock and the highest values for calcareous soils. The concentrations of free  
175 oxides ranged between 1,180 – 22,700 mg kg<sup>-1</sup>.

#### 176 3.2. Soluble U ( $U_{sol}$ )

##### 177 $U_{sol}$ kinetics

178 Figures 1 and 2 show that  $U_{sol}$  decreased rapidly, from the initial addition of 5000 µg kg<sup>-1</sup>, to 2 – 160 µg kg<sup>-1</sup> in  
179 the first 4 days of incubation, probably due to surface complexation and cation exchange reactions (Krupka et  
180 al., 1999). Langmuir (1978) demonstrated that maximum  $UO_2^{2+}$  sorption on minerals occurs a pH 5–8.5; in  
181 acidic organic soils there is greater competition with protons and other metallic cations for adsorption sites.  
182 The initially large and rapid  $U_{sol}$  removal from solution was followed by a slow decline for 6 months and a  
183 subsequent stabilisation, or continued slower decline, for the remainder of the experiment. Earlier studies  
184 reported dual rate kinetics for uranyl sorption on Fe oxides and silica; the first sorption step has been shown  
185 to be complete within minutes (Hsi and Langmuir, 1985; Langmuir, 1978; Tinnacher et al., 2013).  
186 Concentrations of  $U_{sol}$  remaining at the end of the experiment were consistent across all soils (1–40 µg kg<sup>-1</sup>)  
187 and least for near-neutral soils with lower OC.

188 The decline in  $U_{sol}$  fitted the exponential model (Figures 1 and 2) throughout the incubation, especially  
189 over the longer term (Figure S1). The kinetic parameters are plotted in Figure S2 (and Table S1); the depletion  
190 half-times ( $T_{1/2}$ ) ranged between 30 and 250 days suggesting slow  $U_{sol}$  sorption kinetics, following the initial  
191 sorption at 4 days. The slow decline in  $U_{sol}$  has been attributed to inter-particle diffusion, re-distribution to  
192 lower reactivity surface sites, precipitation or other mass transfer-limited processes (Rihs et al., 2004;  
193 Tinnacher et al., 2013). In practical terms, for the soil with the longest  $T_{1/2}$  it would take ca. 5 years to drop  
194 below 1% of starting value. Thus, our data and model fits suggest that some soils showed continued sorption

195 of U beyond 619 days which emphasises the need for studies with extended contact times to inform longer-  
196 term risk assessment calculations.

197 The size of the fraction subject to removal (A) and the persistently soluble fraction (B) appeared to be  
198 pH controlled (Figure S2). With increasing pH, both A and B fractions initially declined, passed through a  
199 minimum around pH 6 and increased again in calcareous soils with pH>7.5. There was a weak negative  
200 relationship between  $T_{1/2}$  and OC. Organic ligands may enhance uranyl adsorption onto Fe oxides forming  
201 ternary  $U^{VI}$ -FA surface complexes (Tinnacher et al., 2013).

### 202 *U<sub>sol</sub> speciation using WHAM7*

203 The proportion of predicted species remained largely unchanged over time and therefore median values for  
204 thirteen time points are reported (Figure S3). At pH<5, solution speciation was dominated by the free uranyl  
205 ion ( $UO_2^{2+}$ ) (30–94%) and uranyl-colloidal FA complexes (4–66%); <20% was predicted to bind to HFO if this  
206 was simulated, and other complexes were minor (<2%). If HFO was not allowed to precipitate in the model  
207 run, there were slightly greater free ion activities because of the absence of complexation with HFO and  $Fe_{sol}$   
208 competition with  $UO_2^{2+}$  for complexation with FA ligands. Greater abundance of uranyl-FA complexes was  
209 reported for organic soils (>10% OC). There was a very strong negative correlation ( $R^2=0.92$ ,  $n=7$ ) between the  
210 abundances of free  $UO_2^{2+}$  and uranyl-FA complexes for acidic soils, suggesting that the presence of organic  
211 ligands may regulate toxicity. Free ion activity peaked for lower organic, acidic soils with OC<10%.

212 Solution speciation between pH 5–7 was dominated by complexation with geocolloids. In soils with  
213  $Fe_{sol} > 100 \mu g L^{-1}$ , 80–99.8%  $U_{sol}$  was bound to HFO, followed by uranyl-FA complexation (up to 15%). The  
214 abundance of free  $UO_2^{2+}$  dropped to <1% with increasing pH. However, when the simulation inhibited  
215 adsorption to colloidal HFO, either because  $Fe_{sol}$  was too low to precipitate or because HFO precipitation was  
216 excluded from the model options, complexation with FA was clearly dominant (60–99%), followed by up to  
217 25% free  $UO_2^{2+}$ , probably reflecting  $Fe_{sol}$ - $U_{sol}$  competition for binding to FA. Uranyl-hydroxides (primarily  
218  $UO_2OH^+$ , 1–13%), carbonate complexes such as  $UO_2CO_3$  and  $UO_2(CO_3)_2^{2-}$  (1–40%) were also predicted in the  
219 absence of HFO. Thus, inclusion of binding to HFO colloids substantially affects apparent  $U_{sol}$  speciation and

220 resultant risk assessments. This is of particular relevance given that free ions are the most bioavailable forms  
221 of metal and are often considered as the best indicator of toxicity (Khan et al., 2011).

222  $U_{\text{sol}}$  in calcareous soils was largely present as carbonate complexes (21–99.8%) as also noted by Krupka  
223 et al. (1999). Where precipitation of colloidal HFO was simulated, 20–99%  $U_{\text{sol}}$  was present as alkaline earth-  
224 uranyl-carbonate complexes, primarily  $\text{Ca}_2\text{UO}_2(\text{CO}_3)_3$ , which rose to 96.9–99.8% in the absence of HFO. In all  
225 the modelling scenarios, uranyl-carbonate complexes made a small contribution (<2%), whilst other species  
226 including free uranyl were absent at this pH (<0.01%) (Figure S3).

### 227 Partition coefficients $K_d$

228 Values of  $K_d$  (Eq. 3) varied widely with ca. 2,000 L kg<sup>-1</sup> for acidic soils, 3,000-40,000 L kg<sup>-1</sup> for neutral soils and  
229 300-20,000 L kg<sup>-1</sup> for calcareous soils (Figure S4). These are within the ranges reported in the literature (Krupka  
230 et al., 1999; Kumar et al., 2019; Sheppard et al., 2007). Values increased slightly within the first few months  
231 reflecting the gradual decrease in  $U_{\text{sol}}$  described above (Figure 2). This time-dependency showed little  
232 dependence on soil properties. The effect of radionuclide-soil/sediment contact time has implications for  
233 radiological risk assessments based upon short-term  $K_d$  values.

234 Multiple regression analysis for the whole dataset did not show significant relationships between soil  
235 properties and the  $K_d$ . This is due to the inconsistent trend with pH around a ‘critical’ pH of 5.5 as noted by  
236 Sheppard et al. (2006). Soil pH controls  $K_d$  through regulating both adsorption strength and (soluble)  
237 complexation processes. The  $K_d$  values in the pH range 3–6 increased with pH ( $\log_{10}(K_d)=0.20(\text{pH})+2.5$ ,  $R^2=0.48$ ,  
238 Figure S5) reflecting increasing uranyl adsorption onto negatively charged soil surfaces such as OC or  
239 sesquioxides. Values of  $K_d$  peaked around pH 6–7 and subsequently declined. A weak negative relationship  
240 between  $K_d$  and pH was evident at pH 6–8 ( $\log_{10}(K_d)=-0.46(\text{pH})+7.0$ ,  $R^2=0.28$ ) reflecting the formation of  
241 aqueous alkaline earth-uranyl-carbonate complexes (Figure S3). This is in line with previous observations on  
242 U solubility (Echevarria et al., 2001; Sheppard et al., 2006).

### 243 **3.3. Chemically exchangeable U ( $U_{\text{exch}}$ )**

244 For soils between pH 3–7,  $U_{\text{exch}}$  concentrations in the early stages of incubation (4 days) were 10–200  
245  $\mu\text{g kg}^{-1}$  (Figure 1b) i.e. <3% of the initially added uranyl concentration. This suggests that the initial rapid  $U_{\text{sol}}$   
246 removal is not associated with simple electrostatically bound, outer-sphere complexation of uranyl ions which  
247 would be exchangeable with hydrated  $\text{Mg}^{2+}$  ions. This is consistent with Hsi and Langmuir (1985) who  
248 demonstrated that uranyl ions are strongly sorbed onto Fe oxides.

249 Soil pH was the main control on  $U_{\text{exch}}$  with a negative relationship for soils between pH 3–7 ( $R^2=0.52$ ;  
250 Figure S6). Slightly greater  $U_{\text{exch}}$  concentrations were seen in acidic organic soils (30–200  $\mu\text{g kg}^{-1}$ ) compared to  
251 near-neutral soils with low humus contents (5–50  $\mu\text{g kg}^{-1}$ ). By contrast,  $U_{\text{exch}}$  concentrations up to 3500  $\mu\text{g kg}^{-1}$   
252 were observed for calcareous soils. Our data indicate that a large proportion (up to 57% of  $U_{\text{total}}$ ) remained  
253 chemically exchangeable over the first 4 months i.e. electrostatically held as weakly sorbed uranyl-carbonate  
254 complexes. This underlines a potential risk to limestone and chalk aquifers given that overlying Rendzina soils  
255 would not retain deposited  $U^{\text{VI}}$ , but rather enhance transport and discharge to the aquifer. Rout et al. (2016)  
256 also found that ca. 50%  $U^{\text{VI}}$  remained chemically exchangeable in calcareous soils after 1 month. Complexation  
257 with carbonate ligands inhibits uranyl adsorption onto Fe oxides (Hsi and Langmuir, 1985; Waite et al., 1994)  
258 although Bargar et al. (1999) showed that  $U^{\text{VI}}$ -carbonate complexes can adsorb on oxide minerals.

259 Median  $U_{\text{exch}}$  data indicate a slow decline over the course of the experiment following the trend in  $U_{\text{sol}}$   
260 (Figure 1). This could be associated with redistribution of sorbed uranyl throughout different reactive surface  
261 sites (Tinnacher et al., 2013) leading to progressive migration to stronger binding sites inaccessible for  
262 chemical exchange.

### 263 **3.4. Isotopically exchangeable U ( $U_{\text{E}}$ )**

#### 264 $U_{\text{E}}$ labile concentrations

265 Uranyl remained largely isotopically exchangeable throughout the experiment (Figures 1 and 3). This  
266 demonstrates that the immediate loss of soluble and exchangeable  $U^{\text{VI}}$  following contamination does not  
267 reflect immobilisation processes. After 365 days, the proportion of isotopically exchangeable  $U_{\text{E}}$  ranged

268 between 50 – 80% of  $U_{\text{total}}$ . After 619 days, 40 – 60% uranyl added was still in dynamic equilibrium with pore  
269 water. These data are broadly consistent with Um et al. (2010), who estimated the isotopically exchangeable  
270 U at 50–60% of the total U for contaminated sediments underlying radioactive waste tanks. Thus, even though  
271 uranyl ions added to soils were rapidly rendered poorly soluble and weakly exchangeable, yet they remain  
272 present in reactive forms despite contrasting soil properties. This contrasts with the literature on U  
273 fractionation which tends to regard water soluble and chemically exchangeable fractions as the ‘potentially  
274 available’ U species in the environment (Rout et al., 2016).

### 275 Predicting $U_E$ solid speciation

276 WHAM7 simulations after 619 days (Figure S7) suggest that labile  $U_E$  was primarily (>95%) adsorbed onto solid  
277 Fe oxides. This suggests that  $U_E$  is probably bound as inner-sphere complexes with Fe oxides, remaining  
278 available for isotopic exchange yet unavailable for ‘indifferent’ cation exchange. Additionally, for acidic organic  
279 soils (OC>10%), 1–5% of  $U_E$  was associated with humic substances in soil. Other pools of  $U_E$  were predicted to  
280 be <2%.

### 281 $U_E$ kinetics

282 Uranium lability ( $U_E$ ) declined over time (Figure 1c) but the majority of soils did not appear to reach equilibrium  
283 (Figure 3). The decreasing trend was very consistent for all soils, despite their contrasting characteristics (pH,  
284 OC,  $Fe_{AM}$ ) and conformed to the exponential model (Figure S1). In contrast to  $U_{\text{sol}}$ , there were no relationships  
285 between the  $U_E$  kinetic parameters (A, B and  $T_{1/2}$ ; Table S2) and soil properties, although average  $T_{1/2}$  for soils  
286 with near-neutral pH were generally lower. The decline in  $U_E$  reflects progressively stronger binding or physical  
287 occlusion of U, but the persistence of the labile fraction B (ca. 3000  $\mu\text{g kg}^{-1}$ ) indicates a limited capacity for  
288 uranyl immobilisation with a long half-life for fixation ( $T_{1/2} = 100\text{--}200$  days). These observations indicate that  
289 the pool of uranyl species able to replenish the soil solution (i) is substantially larger than might be anticipated  
290 from basic chemical extractions; and (ii) declines very slowly suggesting that immobilisation processes  
291 progress at a slow rate regardless of soil characteristics. This is of particular relevance in the context of  
292 radioecological assessments, given that soil solution is the key reservoir for plant uptake.

293 The progressive immobilisation of uranyl may be caused by desorption and re-adsorption processes.  
294 According to the work of Waite et al. (1994) on two-site surface complexation models to predict  $U^{VI}$  binding,  
295 a small population of high-affinity sites exists on the surface of Fe oxides, randomly distributed among a larger  
296 population of relatively low-affinity sites. Thus, uranyl ions may progressively relocate to high-affinity sites  
297 with lower rates of isotopic exchange. Krupka et al. (1999) suggested that  $U^{VI}$  bound to Fe and Mn oxide phases  
298 may not be in isotopic equilibrium with soluble U.

299 Organic matter has also been identified as a potential sink for  $U^{VI}$ , although the underlying mechanisms  
300 are still unclear (Krupka et al., 1999) as is the involvement of abiotic or biotic reduction processes (Cumberland  
301 et al., 2016). Microbial reduction of  $U^{VI}$  leading to formation of immobile  $U^{IV}$  forms has been extensively  
302 documented (Newsome et al., 2014). However, we observed consistent  $Fe_{sol}$  and  $Mn_{sol}$  concentrations over  
303 the course of the experiment (Izquierdo et al. 2019), which suggests that the electrochemical status of the 20  
304 soils remained largely unchanged. Thus, any reductive processes leading to formation of  $U^{IV}$  may be limited to  
305 microenvironments following local exhaustion of  $O_2$  within soil pore microsites, and it may not have  
306 progressed much further down the redox ladder, whilst the bulk of the soil remained aerated. In addition,  
307 microbially-mediated  $U^{VI}$  reduction to  $U^{IV}$  and subsequent fixation would be enhanced by decomposable  
308 organic matter that can fuel bacterial activity. However, there was no clear evidence for kinetically enhanced  
309 fixation rates in organic soils (Figure 3a). Our findings suggest that bioreduction processes play a marginal role  
310 in the kinetics of labile  $U^{VI}$ . Studies on organic soils naturally enriched in U by Fuller et al. (2020) and  
311 Regenspurg et al. (2010) have demonstrated that U was largely complexed with soil organic matter as  $U^{VI}$   
312 despite reducing conditions; binding to organic matter appeared to prevent  $U^{VI}$  bioreduction. Similarly, Burgos  
313 et al. (2007) suggested that complexation of  $U^{VI}$  with humic substances may interrupt electron transport to  $U^{VI}$   
314 thereby decreasing the potential for reduction. Thus, it is more likely that  $U_E$  removal in high organic soils  
315 reflects abiotic fixation pathways in which rapid, initial adsorption is followed by re-organisation to more  
316 stable complexes (Krupka et al., 1999; Regenspurg et al., 2010).

317 Although carbonate ligands inhibit U adsorption, the trends in  $U_E$  (Figure 3c) also suggest transfer to  
318 non-labile forms in calcareous soils, as reported by Cumberland et al. (2016) and Elless and Lee (1998).  
319 Synchrotron-based studies by Elzinga et al. (2004) and Rihs et al. (2004) showed surface complexation of  
320 uranyl-carbonate species via inner-sphere bonding of  $U^{VI}$  with a surface carbonate group, primarily in  
321 monodentate coordination. Following  $U^{VI}$  adsorption, calcite dissolution and re-precipitation may then result  
322 in the slow incorporation of  $U^{VI}$  into  $CaCO_3$  in non-labile forms.

### 323 Partitioning between labile adsorbed $U^{VI}$ and free $UO_2^{2+}$ ions in solution: $K_d^L$

324 Solid-liquid partition coefficients ( $K_d^L$ ) based on isotopically exchangeable  $U^{VI}$  and free uranyl in solution  
325 provide a more mechanistically rigorous expression of the partitioning of geochemically reactive  $U^{VI}$  than  
326 conventional  $K_d$  expressions. Free uranyl ions are the form most readily accumulated by plant roots (Mitchell  
327 et al., 2013) and probably the best indicator of potential toxicity, although  $U^{VI}$ -carbonate complexes may also  
328 be bioavailable (Vandenhove et al., 2007b). Values of the labile  $K_d^L$  are substantially greater than standard  
329 solid-to-liquid  $K_d$  (Figure S4). Values of  $\log_{10}K_d^L$  ranged from 6 – 14 primarily reflecting the strong effect of soil  
330 pH ( $R^2=0.93$ ; Figure 4) on binding of  $UO_2^{2+}$  ions to geocolloids. Values of the conventional  $K_d$  showed little  
331 variation with pH as the stronger binding at high pH was effectively offset by the formation of soluble U-  
332 carbonate complexes.

### 333 Predicting $U_{sol}$ from $U_E$

334 Prediction of  $U_{sol}$  concentrations from soil properties and labile  $U_E$  using WHAM7 was attempted. Goodness  
335 of fit was assessed by calculating Residual Standard Deviation (RSD). Using  $Fe_{FREE}$  and  $Mn_{FREE}$  as potential  
336 adsorption surfaces, together with HA, underestimated  $U_{sol}$  (RSD=1.20), probably due to overestimating the  
337 surface area available for uranyl binding. Improved predictions were obtained when (i) HA,  $Fe_{AM}$  and  $Mn_{AM}$   
338 estimates were used as particulate active binding phases and (ii) formation of colloidal HFO with chemically  
339 active surface was allowed (RSD=0.74, Figure S7); the majority of  $U_{sol}$  data fell along the 1:1 line and within  
340  $\pm 1RSD$ .

341 Omitting colloidal HFO in the modelling options resulted in poor prediction of  $U_{\text{sol}}$  (RSD=2.24, Figure  
342 S8). There was a systematic bias in the predictions, which widened in near-neutral soils where  $U_{\text{sol}}$  was low  
343 and primarily driven by complexation with HFO/FA colloids. Predictions of  $U_{\text{sol}}$  were more accurate when  
344 complexation reactions with colloidal FA or HFO ligands were marginal: (i) in acidic soils in which aqueous  $U^{\text{VI}}$   
345 is essentially as free ( $UO_2^{2+}$ ); and (ii) in calcareous soils, dominated by complexation with carbonate ligands.  
346 This emphasises the relevance of colloidal complexes in controlling  $U^{\text{VI}}$  solubility, particularly within pH 4 – 7.

## 347 **4. CONCLUSIONS**

348 Following contamination,  $U^{\text{VI}}$  was rapidly removed from solution and was bound to oxides in soil. This was  
349 followed by a slower decline in soluble uranyl following an offset exponential kinetic model. Our data suggest  
350 that short-term experiments may not be used reliably to predict long-term solubility and  $K_d$  values, which has  
351 practical significance in risk assessment calculations for facilities such as radioactive waste repositories.

352 Uranium remained more soluble in calcareous soils due to complexation with carbonate ligands; data  
353 and model predictions suggest that a large proportion of  $U^{\text{VI}}$  in calcareous soils is electrostatically held as  
354 weakly sorbed uranyl-carbonate complexes. These weakly bonded fractions are particularly relevant in some  
355 environments; Rendzina soils in calcareous terrains would be inefficient at retaining deposited  $U^{\text{VI}}$  and would  
356 not prevent, but rather enhance, transport, dispersion and discharge to the underlying aquifer.

357 The comparison between solubility and chemical exchangeability data with isotopic exchangeability  
358 provided evidence of the binding strength of uranyl onto soils. Despite the low solubility and exchangeability,  
359 the added uranyl was almost fully labile after 4 days. Thus, whilst uranyl sorption is rapid and strongly buffered  
360 by Fe oxides present in soil,  $U^{\text{VI}}$  is still reversibly held and geochemically reactive. The kinetics of labile U is  
361 remarkably similar between soils and the time trends are small. For the majority of soils, added U was still  
362 undergoing net sorption after 600 days and that ca. 50% uranyl added was still in dynamic equilibrium with  
363 pore water after this contact time. Modelled kinetic parameters suggest a timeframe of typically 100–200 days  
364 to reduce the initially labile  $U_E$  by half. Crucially, these findings indicate that the pool of uranyl species able to

365 replenish the soil solution through dissolution, precipitation, de-sorption or dissociation equilibrium reactions  
366 (i) is substantially larger than might be anticipated from chemical extractions typically used in soil science, (ii)  
367 declines very slowly suggesting that the processes and transformations conducive to uranyl transfer to an  
368 intractable sink progress at a slow rate regardless of soil characteristics. This is of particular relevance in the  
369 context of radioecological assessments, given that soil solution is the key reservoir for plant uptake.

## 370 **ACKNOWLEDGMENTS**

371 This work was carried out within the TREE (Transfer-Exposure-Effects) consortium within the Radioactivity and  
372 the Environment (RATE) programme, funded jointly by the Natural Environment Research Council, Radioactive  
373 Waste Management Ltd. and the Environment Agency (grant no. NE/L000504/1). We thank the numerous  
374 individuals and agencies who gave permission to sample soils.

## 375 **REFERENCES**

- 376 Alloway, B.J. (2012) Heavy metals in soils: trace metals and metalloids in soils and their bioavailability. Springer  
377 Science & Business Media.
- 378 Bargar, J.R., Reitmeyer, R. and Davis, J.A. (1999) Spectroscopic Confirmation of Uranium(VI)-Carbonato  
379 Adsorption Complexes on Hematite. *Environ. Sci. Technol.* 33, 2481-2484.
- 380 Bond, D.L., Davis, J.A. and Zachara, J.M. (2007) Uranium (VI) release from contaminated vadose zone  
381 sediments: Estimation of potential contributions from dissolution and desorption. *Developments in Earth  
382 and Environmental Sciences* 7, 375-416.
- 383 Buekers, J., Degryse, F., Maes, A. and Smolders, E. (2008) Modelling the effects of ageing on Cd, Zn, Ni and Cu  
384 solubility in soils using an assemblage model. *Eur. J. Soil Sci.* 59, 1160-1170.
- 385 Burgos, W.D.S.J.M.D., B.A.; E.E. Roden, J.J. Stone, K.M. Kemner, S.D. Kelly (2007) Soil humic acid decreases  
386 biological uranium(vi) reduction by *Shewanella putrefaciens* CN32. *Environ. Eng. Sci.* 24, 755-761.
- 387 Crawford, S.E., Lofts, S. and Liber, K. (2017) The role of sediment properties and solution pH in the adsorption  
388 of uranium(VI) to freshwater sediments. *Environ. Pollut.* 220, 873-881.
- 389 Cumberland, S.A., Douglas, G., Grice, K. and Moreau, J.W. (2016) Uranium mobility in organic matter-rich  
390 sediments: A review of geological and geochemical processes. *Earth-Sci. Rev.* 159, 160-185.
- 391 Echevarria, G., Sheppard, M.I. and Morel, J. (2001) Effect of pH on the sorption of uranium in soils. *J. Environ.  
392 Radioactiv.* 53, 257-264.
- 393 Elless, M.P. and Lee, S.Y. (1998) Uranium Solubility of Carbonate-Rich Uranium-Contaminated Soils. *Water,  
394 Air, Soil Pollut.* 107, 147-162.
- 395 Elzinga, E.J., Tait, C.D., Reeder, R.J., Rector, K.D., Donohoe, R.J. and Morris, D.E. (2004) Spectroscopic  
396 investigation of U(VI) sorption at the calcite-water interface. *Geochim. Cosmochim. Acta* 68, 2437-2448.

397 Fuller, A.J., Leary, P., Gray, N.D., Davies, H.S., Mosselmans, J.F.W., Cox, F., Robinson, C.H., Pittman, J.K.,  
398 McCann, C.M., Muir, M., Graham, M.C., Utsunomiya, S., Bower, W.R., Morris, K., Shaw, S., Bots, P., Livens,  
399 F.R. and Law, G.T.W. (2020) Organic complexation of U(VI) in reducing soils at a natural analogue site:  
400 Implications for uranium transport. *Chemosphere* 254, 126859.

401 Gavrilescu, M., Pavel, L.V. and Cretescu, I. (2009) Characterization and remediation of soils contaminated with  
402 uranium. *J. Hazard. Mater.* 163, 475-510.

403 Hamon, R.E., Parker, D.R. and Lombi, E. (2008) Chapter 6 Advances in Isotopic Dilution Techniques in Trace  
404 Element Research: A Review of Methodologies, Benefits, and Limitations, in: Donald, L.S. (Ed.), *Advances*  
405 *in Agronomy*. Academic Press, pp. 289-343.

406 Hsi, C.-k.D. and Langmuir, D. (1985) Adsorption of uranyl onto ferric oxyhydroxides: Application of the surface  
407 complexation site-binding model. *Geochim. Cosmochim. Acta* 49, 1931-1941.

408 Izquierdo, M., Bailey, E.H., Crout, N.M.J., Sanders, H.K., Young, S.D. and Shaw, G.G. (2019) Kinetics of <sup>99</sup>Tc  
409 speciation in aerobic soils. *J. Hazard. Mater.*, 121762.

410 Khan, M.S., Zaidi, A., Goel, R. and Musarrat, J. (2011) *Biomanagement of metal-contaminated soils*. Springer  
411 Science & Business Media.

412 Kohler, M., Curtis, G.P., Meece, D.E. and Davis, J.A. (2004) Methods for Estimating Adsorbed Uranium(VI) and  
413 Distribution Coefficients of Contaminated Sediments. *Environ. Sci. Technol.* 38, 240-247.

414 Krupka, K.M., Kaplan, D., Whelan, G., Serne, R. and Mattigod, S. (1999) Understanding variation in partition  
415 coefficient, K<sub>d</sub>, values, in: 402-R-99-004B, E. (Ed.), *Volume II: Review of Geochemistry and Available K<sub>d</sub>*  
416 *Values, for Cadmium, Cesium, Chromium, Lead, Plutonium, Radon, Strontium, Thorium, Tritium (3H), and*  
417 *Uranium*. EPA. United States Environmental Protection Agency.

418 Kumar, A., Rout, S., Pulhani, V. and Kumar, A.V. (2019) A review on distribution coefficient (K<sub>d</sub>) of some  
419 selected radionuclides in soil/sediment over the last three decades. *J. Radioanal. Nucl. Chem.*

420 Langmuir, D. (1978) Uranium solution-mineral equilibria at low temperatures with applications to sedimentary  
421 ore deposits. *Geochim. Cosmochim. Acta* 42, 547-569.

422 Lofts, S., Tipping, E. (2011). Assessing WHAM/Model VII against field measurements of free metal ion  
423 concentrations: Model performance and the role of uncertainty in parameters and inputs. *Environ. Chem.*  
424 8, 501-516.

425 Lofts, S., Fevrier, L., Horemans, N., Gilbin, R., Bruggeman, C. and Vandenhove, H. (2015) Assessment of co-  
426 contaminant effects on uranium and thorium speciation in freshwater using geochemical modelling. *J.*  
427 *Environ. Radioactiv.* 149, 99-109.

428 Lottermoser, B.G., Schnug, E. and Haneklaus, S. (2011) Cola soft drinks for evaluating the bioaccessibility of  
429 uranium in contaminated mine soils. *Sci. Total Environ.* 409, 3512-3519.

430 Manoj, S., Thirumurugan, M. and Elango, L. (2019) Determination of distribution coefficient of uranium from  
431 physical and chemical properties of soil. *Chemosphere*, 125411.

432 Midwood, A.J. (2007) Stable Isotope Methods for Estimating the Labile Metal Content of Soils, in: Willey, N.  
433 (Ed.), *Phytoremediation. Methods and Reviews Humana Press*, pp. 149-159.

434 Mitchell, N., Pérez-Sánchez, D. and Thorne, M.C. (2013) A review of the behaviour of U-238 series  
435 radionuclides in soils and plants. *J. Radiol. Prot.* 33, R17-R48.

436 Mossa, A.-W., Bailey, E.H., Usman, A., Young, S.D. and Crout, N.M.J. (2020) The impact of long-term biosolids  
437 application (>100 years) on soil metal dynamics. *Sci. Total Environ.*, 137441.

438 Newsome, L., Morris, K. and Lloyd, J.R. (2014) The biogeochemistry and bioremediation of uranium and other  
439 priority radionuclides. *Chem. Geol.* 363, 164-184.

- 440 Olsen, R. V., Roscoe E.J.R., *Methods of Soil Analysis: Part 2—Chemical and Microbiological Properties*, ed. A. L.  
441 Page, R. H. Miller and D. R. Keeney, Madison, WI, 1982, pp. 301–312
- 442 Regenspurg, S., Margot-Roquier, C., Harfouche, M., Froidevaux, P., Steinmann, P., Junier, P. and Bernier-  
443 Latmani, R. (2010) Speciation of naturally-accumulated uranium in an organic-rich soil of an alpine region  
444 (Switzerland). *Geochim. Cosmochim. Acta* 74, 2082-2098.
- 445 Rihs, S., Sturchio, N.C., Orlandini, K., Cheng, L., Teng, H., Fenter, P. and Bedzyk, M.J. (2004) Interaction of Uranyl  
446 with Calcite in the Presence of EDTA. *Environ. Sci. Technol.* 38, 5078-5086.
- 447 Rout, S., Kumar, A., Ravi, P.M. and Tripathi, R.M. (2016) Understanding the solid phase chemical fractionation  
448 of uranium in soil and effect of ageing. *J. Hazard. Mater.* 317, 457-465.
- 449 Schwertmann, U. (1973) Use of oxalate for Fe extraction from soils. *Can. J. Soil Sci.* 53, 244-246.
- 450 Sheppard, M.I., Sheppard, S.C. and Grant, C.A. (2007) Solid/liquid partition coefficients to model trace element  
451 critical loads for agricultural soils in Canada. *Can. J. Soil Sci.* 87, 189-201.
- 452 Sheppard, S., Long, J., Sanipelli, B. and Sohlenius, G. (2009) Solid/liquid partition coefficients ( $K_d$ ) for selected  
453 soils and sediments at Forsmark and Laxemar-Simpevarp, in: 1402-3091, I., R-09-27, S.R. (Eds.). Swedish  
454 Nuclear Fuel and Waste Management Co.
- 455 Sheppard, S.C., Sheppard, M.I., Tait, J.C. and Sanipelli, B.L. (2006) Revision and meta-analysis of selected  
456 biosphere parameter values for chlorine, iodine, neptunium, radium, radon and uranium. *J. Environ.*  
457 *Radioactiv.* 89, 115-137.
- 458 Tinnacher, R.M., Nico, P.S., Davis, J.A. and Honeyman, B.D. (2013) Effects of Fulvic Acid on Uranium(VI)  
459 Sorption Kinetics. *Environ. Sci. Technol.* 47, 6214-6222.
- 460 Tye, A.M., Young, S., Crout, N.M.J., Zhang, H., Preston, Bailey, E., Davison, W., McGrath, S.P., Paton G. I. and  
461 Kilham, K. (2002) Predicting arsenic solubility in contaminated soils using isotopic dilution techniques.  
462 *Environ. Sci. Technol.* 36, 982–988.
- 463 Tye, A.M., Young, S., Crout, N.M.J., Zhang, H., Preston, S., Zhao, F.J. and McGrath, S.P. (2004) Speciation and  
464 solubility of Cu, Ni and Pb in contaminated soils. *Eur. J. Soil Sci.* 55, 579-590.
- 465 Um, W., Icenhower, J.P., Brown, C.F., Serne, R.J., Wang, Z., Dodge, C.J. and Francis, A.J. (2010) Characterization  
466 of uranium-contaminated sediments from beneath a nuclear waste storage tank from Hanford,  
467 Washington: Implications for contaminant transport and fate. *Geochim. Cosmochim. Acta* 74, 1363-1380.
- 468 Vandenhove, H., Van Hees, M., Wouters, K. and Wannijn, J. (2007a). Can we predict uranium bioavailability  
469 based on soil parameters? Part 1: Effect of soil parameters on soil solution uranium concentration.  
470 *Environ. Pollut.* 145, 587-595.
- 471 Vandenhove, H., Van Hees, M., Wannijn, J., Wouters, K. and Wang, L. (2007b) Can we predict uranium  
472 bioavailability based on soil parameters? Part 2: soil solution uranium concentration is not a good  
473 bioavailability index. *Environ. Pollut.* 145, 577-586.
- 474 Vandenhove, H., Vanhoudt, N., Duquène, L., Antunes, K. and Wannijn, J. (2014) Comparison of two sequential  
475 extraction procedures for uranium fractionation in contaminated soils. *J. Environ. Radioactiv.* 137, 1-9.
- 476 Waite, T., Davis, J., Payne, T., Waychunas, G. and Xu, N. (1994) Uranium (VI) adsorption to ferrihydrite:  
477 Application of a surface complexation model. *Geochim. Cosmochim. Acta* 58, 5465-5478.
- 478 Young, S.D., Zhang, H., Tye, A.M., Maxted, A., Thums, C. and Thornton, I. (2005) Characterizing the availability  
479 of metals in contaminated soils. I. The solid phase: sequential extraction and isotopic dilution. *Soil Use*  
480 *Manage.* 21, 450-458.

481 Young, S.D., Crout, N., Hutchinson, J., Tye, A., Tandy, S. and Nakhone, L. (2006) Techniques for measuring  
482 attenuation: isotopic dilution methods in: R. Hamon, M.M., E. Lombi (Ed.), Natural Attenuation of Trace  
483 Element Availability in Soils CRC Press, Boca Raton, FL, pp. 19-55.

**Table 1.** Location and general properties of the soils in this study, listed in order of land use. Bdl denotes below the detection limit.

code	land use	Latitude	Longitude	%	%	pH	total concentrations mg kg <sup>-1</sup>			Free amorphous oxides mg kg <sup>-1</sup>			Total free oxides mg kg <sup>-1</sup>			incubation moisture content	
							inorg C	organic C	U (native)	Al	Mn	Fe	Al	Mn	Fe	Al	Mn
CO-A	arable	52° 49' 36.9" N	1° 13' 35.08" W	Bdl	2.3	6.37	1799	26707	508	20965	633	317	3386	751	356	9372	9
EV-A	arable	52° 50' 39.43" N	1° 11' 25.83" W	0.043	2.6	6.04	2336	43275	934	34961	1244	622	4233	1245	736	14217	12
NP-A	arable	52° 51' 38.39" N	1° 7' 30.47" W	Bdl	1.7	6.76	1269	15873	501	17725	637	277	2103	617	331	7531	9
SR-A	arable	52° 51' 3.19" N	0°40'35.01"W	5.33	3.8	7.77	1464	23207	682	22515	1333	232	1181	1176	364	12425	9
WK-A	arable	52° 49' 47.96" N	1° 14' 24.12" W	Bdl	2.4	5.31	1458	19815	645	29614	762	404	3688	842	414	9270	13
WS-A	arable	52° 51' 9.31" N	1° 7' 36.4" W	0.74	2.6	7.71	2181	42149	1037	33255	604	349	1205	456	431	7166	14
BH-G	grassland	52° 48'24.77"N	1°23'58.86"W	1.16	6.2	7.36	4926	27237	4451	30438	1487	3143	5184	1110	3525	14599	20
DY-G	grassland	53° 18'55.30"N	1° 36'1.37"W	Bdl	11.4	3.90	722	15841	43	6925	863	18	2264	1089	36	5563	31
FD-G	grassland	52° 49' 54.13" N	1° 13' 35.92" W	Bdl	5.7	6.19	3177	57058	1053	52789	1626	505	8148	1130	679	18387	24
SB-G	grassland	52° 47' 23.53" N	1° 27' 58.07" W	Bdl	5.0	6.02	1710	22103	460	13775	1181	289	5436	1294	331	10073	15
SR-G	grassland	52° 51' 0.83" N	0° 40' 39.93"W	0.38	5.7	7.04	1651	36862	874	50808	1985	529	3893	1956	666	22668	22
TK-G	grassland	52° 47' 36.62" N	1° 28' 29.94" W	Bdl	6.3	5.32	2825	40942	303	25256	2041	160	7069	1904	165	11484	20
BC-M	moorland	53° 12'44.29"N	1° 5'33.07"W	bdl	5.5	4.18	1477	21124	77	16124	876	6	4841	995	22	7850	15
DY-M	moorland	53° 18'42.34"N	1° 35'59.93"W	Bdl	38.6	3.46	1037	10439	43	5759	2430	18	3421	2987	24	3940	36
BH-W	woodland	52° 48'23.80"N	1°24'5.18"W	2.83	7.5	7.47	2245	23500	2724	25395	880	1398	3126	675	1535	10514	16
BY-W	woodland	52° 49' 42.66" N	1° 27' 51.02" W	Bdl	10.6	3.41	2461	30226	141	22966	1347	55	6978	1634	90	14285	21
IH-W	woodland	52° 44' 54.74" N	1° 17' 51.89" W	Bdl	9.5	3.88	1905	27554	185	18013	1604	60	4178	1826	95	9496	20
PE-W	woodland	53° 12'44.41"N	1° 5'53.23"W	Bdl	7.1	3.82	1076	18022	91	7655	670	38	1806	756	55	4720	12
SR-W	woodland	52° 50' 58.28" N	0°40' 33.61"W	3.75	5.2	8.00	1180	28029	694	25431	1813	321	1650	-	-	-	13
WK-W	woodland	52° 49' 51.48" N	1° 14' 17.8" W	Bdl	24.4	3.87	838	11025	233	13202	1365	143	3578	1444	198	5778	37

## FIGURE CAPTIONS

**Figure 1.** Changes in the concentrations of U in the soluble (a), chemically exchangeable (b), and labile or isotopically exchangeable pools (c) over the course of 619 days incubation in 20 soils. Circles and whiskers denote median values and interquartile (25–75%) range for all soils within the specified pH interval categories, respectively. For  $U_{\text{sol}}$  and  $U_{\text{E}}$  median values, single exponential models have been fitted. **The red arrow denotes the concentration of natural U added to soils.**

**Figure 2.** Kinetics of removal of  $U_{\text{sol}}$  from the soluble (0.01 M  $\text{KNO}_3$  extractable) pool in acidic ( $\text{pH}<5$ ) (a), near-neutral ( $\text{pH } 5\text{--}7$ ) (b) and calcareous ( $\text{pH}<7$ ) (c) soils over the course of 619 days. The points are experimental data through which an offset single exponential model has been fitted. Soil codes are listed in Table 1.

**Figure 3.** Kinetics of the isotopically exchangeable (labile)  $U_{\text{E}}$  in acidic ( $\text{pH}<5$ ) (a), near-neutral ( $\text{pH } 5\text{--}7$ ) (b) and calcareous ( $\text{pH}<7$ ) (c) soils over the course of 619 days. The points are experimental data through which an offset single exponential model has been fitted. Soil codes are listed in Table 1.

**Figure 4.** Relationship between soil pH and the labile  $\log K_{\text{d}}^{\text{L}}$  **after 619 days incubation.**

Figure 1

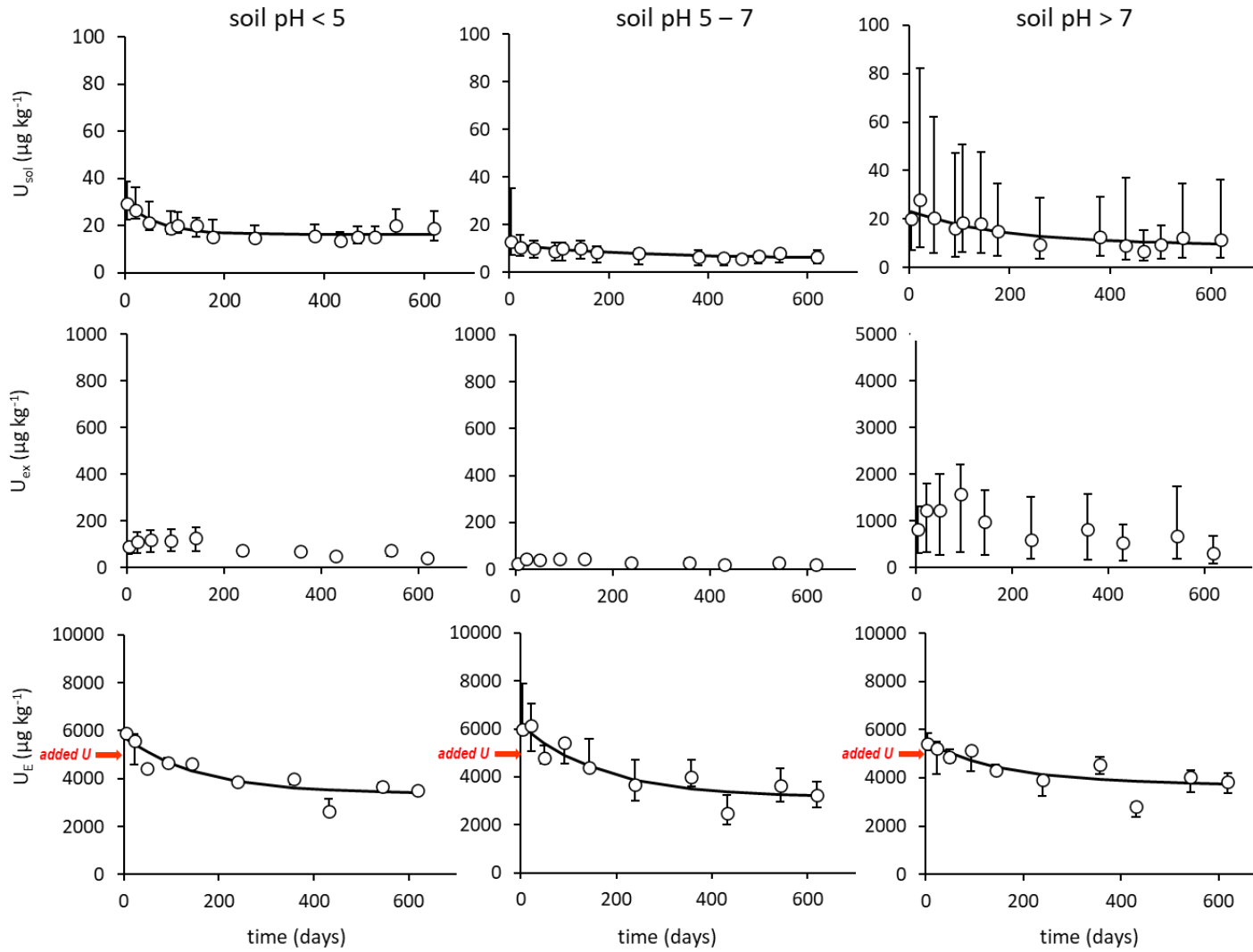


Figure 2

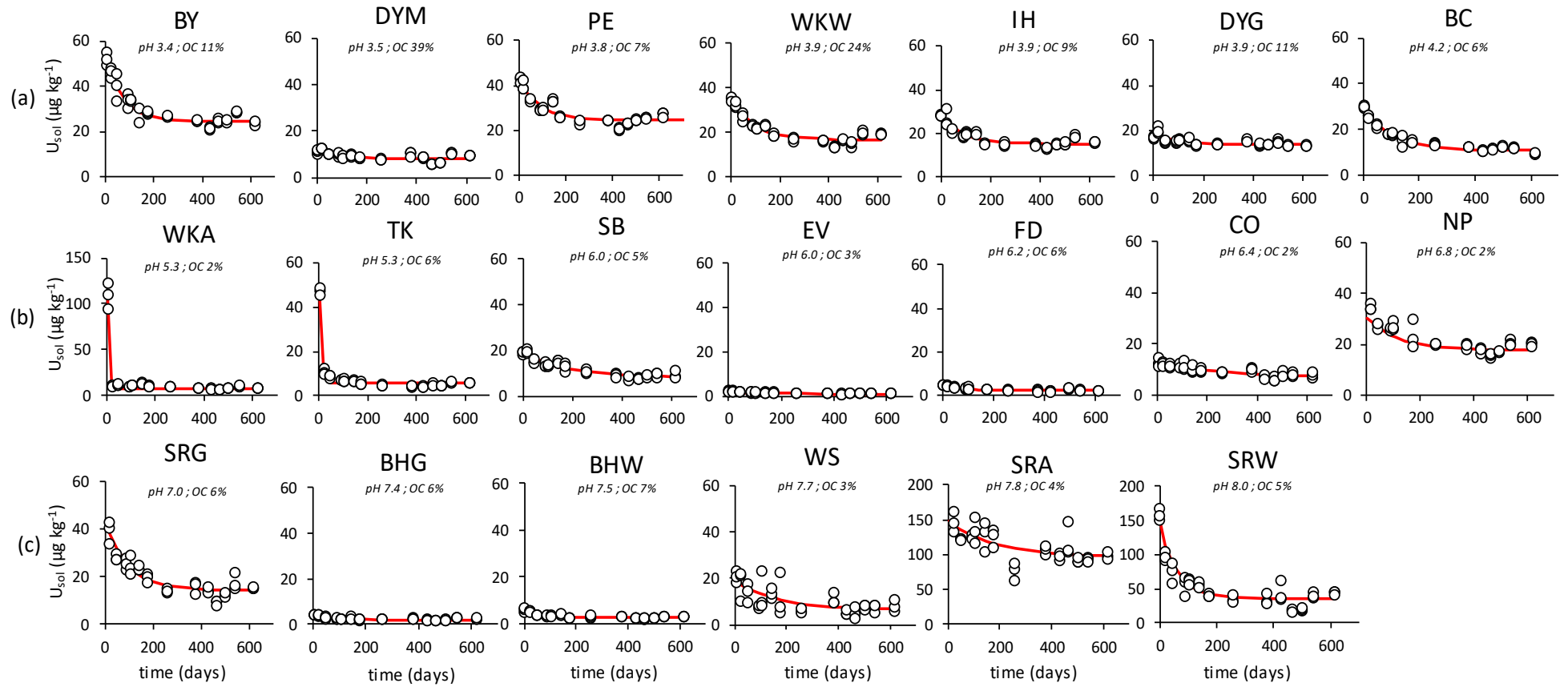


Figure 3

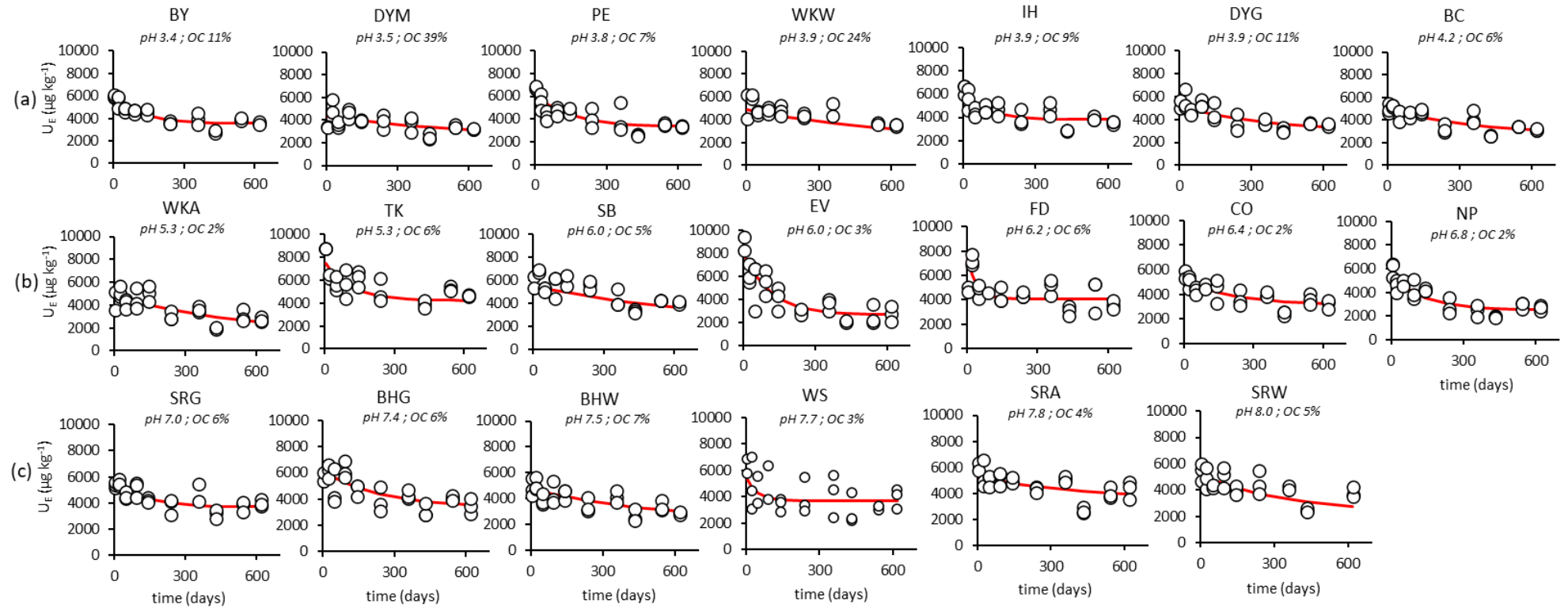
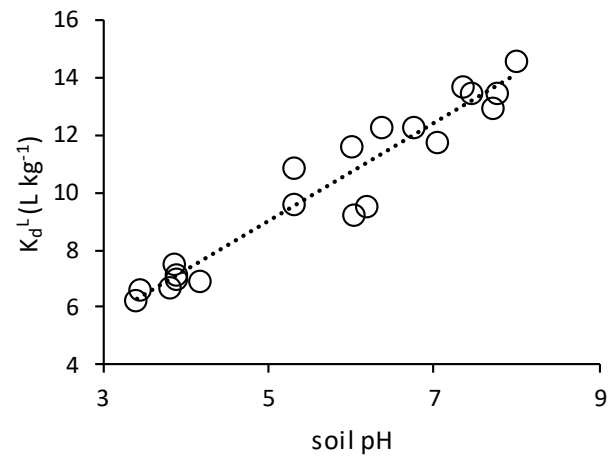


Figure 4



---

## Kinetics of uranium(VI) lability and solubility in aerobic soils

M. Izquierdo<sup>ab\*</sup>, S.D. Young<sup>a</sup>, E.H. Bailey<sup>a</sup>, N.M.J. Crout<sup>a</sup>, S. Lofts<sup>c</sup>, S.R. Chenery<sup>d</sup> and G. Shaw<sup>a</sup>

<sup>a</sup>School of Biosciences, University of Nottingham, Sutton Bonington Campus, Loughborough, LE12 5RD, United Kingdom

<sup>b</sup>Institute of Environmental Assessment and Water Research, 18-26 Jordi Girona, Barcelona 08034, Spain

<sup>c</sup>UK Centre for Ecology and Hydrology, Lancaster Environment Centre, Library Avenue, Bailrigg, Lancaster, LA1 4AP, United Kingdom

<sup>d</sup>British Geological Survey, Environmental Science Centre, Keyworth, Nottingham, NG12 5GG, United Kingdom

\*corresponding author: maria.izquierdo@idaea.csic.es Tel. +34934006146

---

### Supplementary Information

---

**Figure S1.** The comparison between observed and modelled  $U_{\text{sol}}$  (a) and  $U_{\text{E}}$  (b) using Eq.5 for the full dataset.

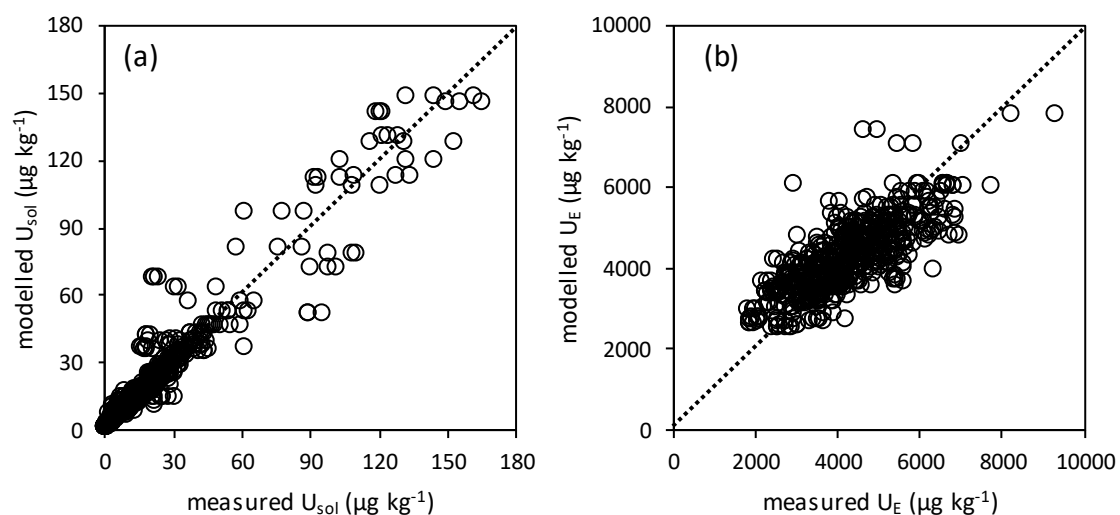


**Figure S2.** Relationships between soil pH, organic C (OC), free iron oxides  $Fe_{AM}$  and modelled kinetic parameters for  $U_{soil}$  including A, B and  $T_{1/2}$ . Several outliers have been identified.

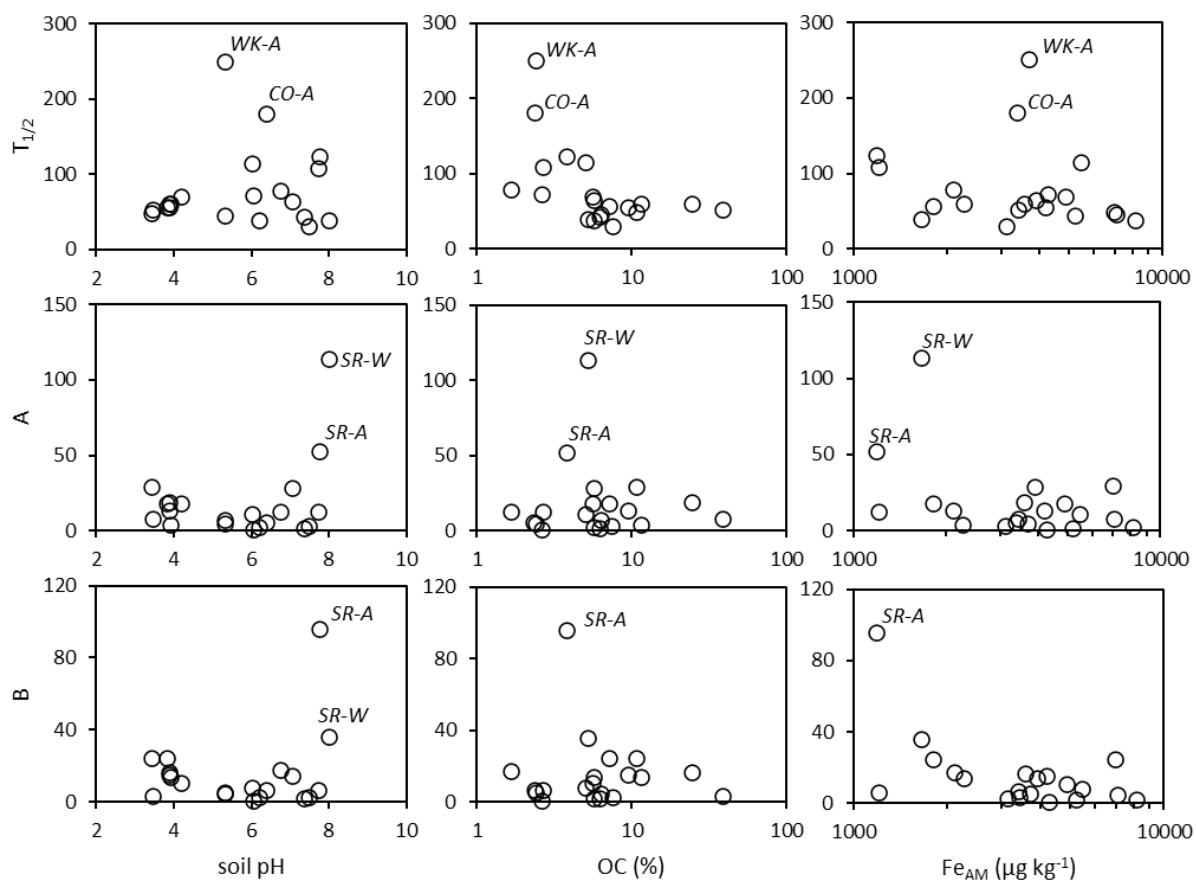


**Figure S3.** Predicted distribution of aqueous uranyl species across the pH range in two scenarios i.e. preventing and enabling formation of colloidal HFO with surface charge. Model outputs are plotted as defined groups of species including free ion, uranyl complexed with a range of inorganic aqueous ligands and bound to geocolloids (FA, HFO).

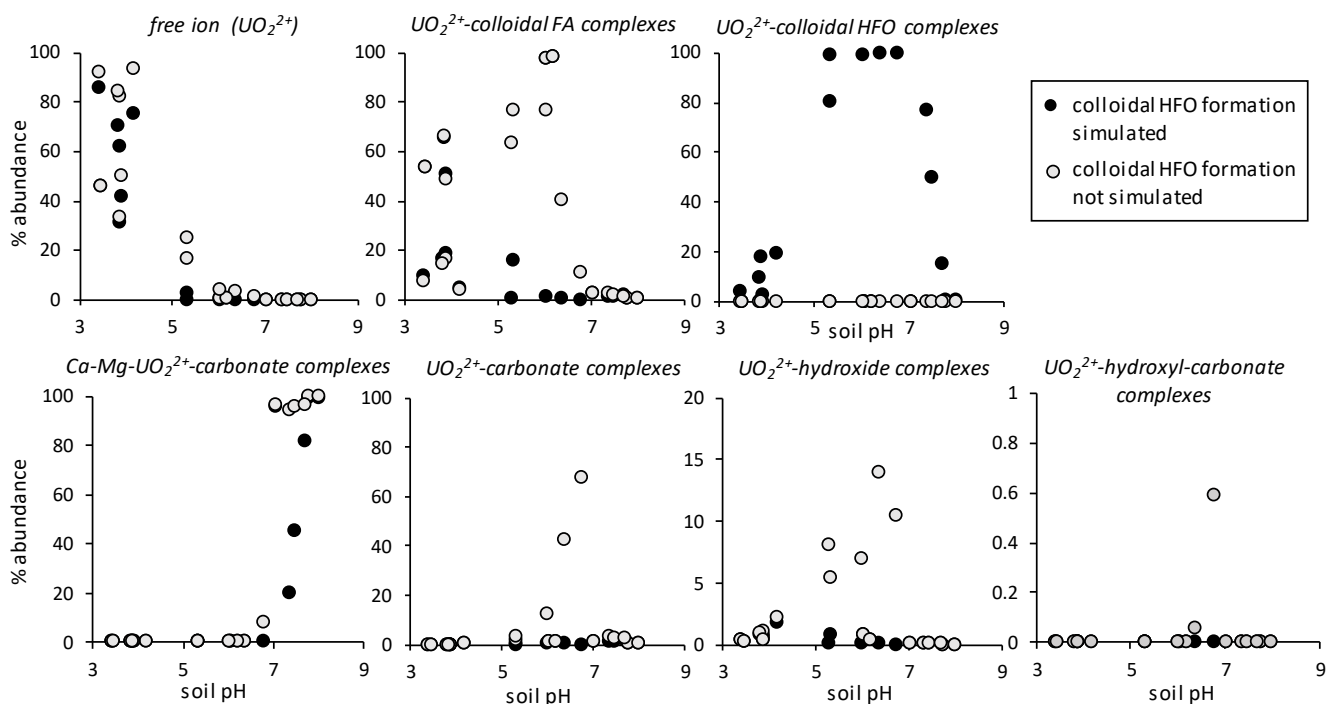


**Figure S4.** Changes in measured  $K_d$  values over the course of the incubation experiment.  $K_d$  denotes the partition coefficient between the total U concentration in soil and  $U_{sol}$  measured in 0.01M  $KNO_3$  extracts (Eq.3).  $K_d^L$  denotes the partition coefficient between the adsorbed and isotopically exchangeable U and the uranyl present as free ion in the 0.01M  $KNO_3$  extracts (Eq. 4).

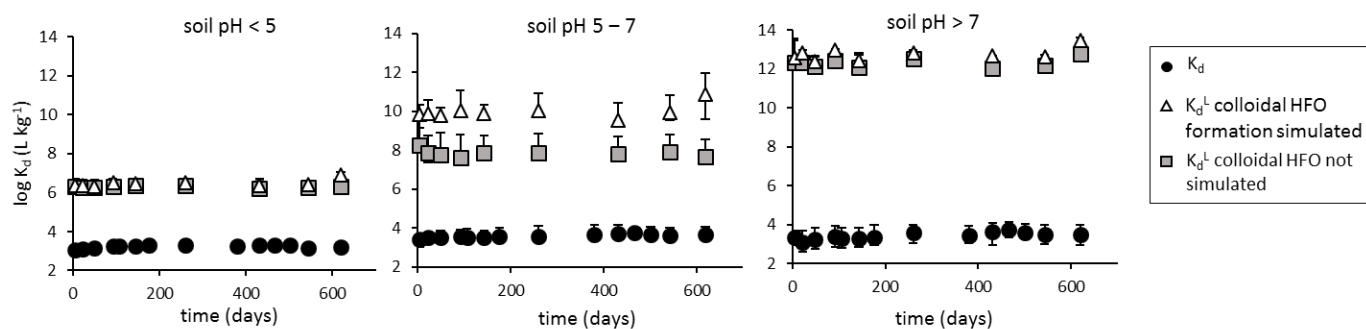


**Figure S5.** Relationships between U  $K_d$  and selected soil properties including (a) soil pH, and two linear relationships for pH 3 – 6 ( $R^2=0.49$ ) and pH 6 – 8 ( $R^2=0.28$ ); (b) total organic C content in soil; and (c) concentration of free, amorphous Fe oxides and a linear relationship ( $R^2=0.30$ ).

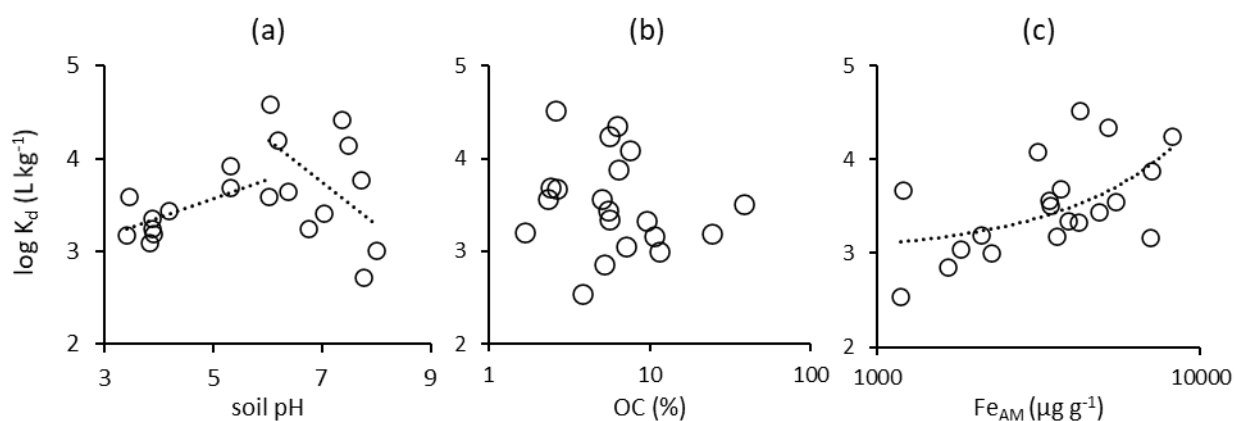


**Figure S6.** Relationship between soil pH and the chemical exchangeability of U after 4 days incubation. Data split in two subsets i.e. acidic + near neutral (pH < 7; linear relationship  $R^2=0.53$ ) and calcareous soils (pH > 7,  $R^2=0.30$ ).

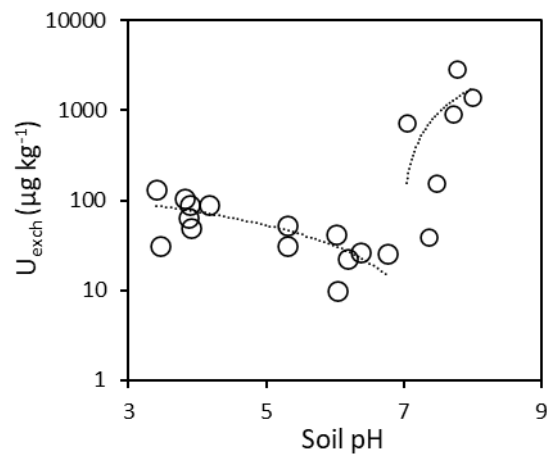


**Figure S7.** WHAM7 outputs using labile  $U_E$  after 619 days incubation as input data: (a) Comparison between observed and predicted  $U_{sol}$  concentrations at 619 days. The solid line is the 1:1 line whilst dashed lines represent  $\pm 1RSD$ . (b) Proportion of the solid phases that the labile pool of  $U_E$  are associated with. Modelling options includes humic substances and  $Fe_{AM}$  and  $Mn_{AM}$  as particulate binding phases, and  $Fe_{sol}$  and FA as colloidal binding phases. Outliers (i.e. beyond  $\pm 1RSD$ ) correspond to low  $U_{sol}$ , low  $Fe_{sol}$  near neutral EV-A and FD-G soils.

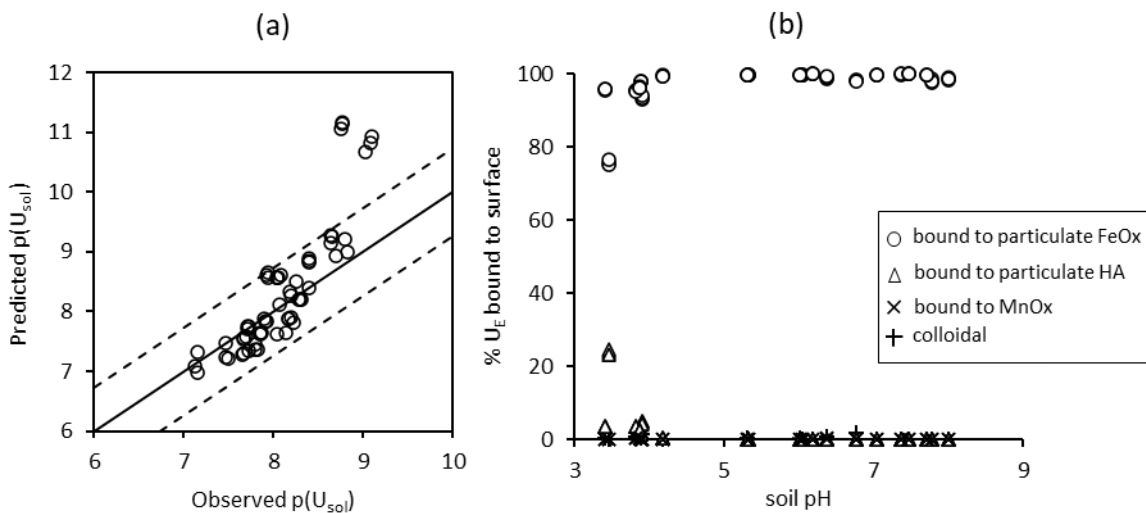


**Figure S8.** Comparison between observed and predicted concentrations of  $U_{sol}$  using WHAM7 when colloidal HFO is not allowed to precipitate in the modelling options. The solid line represents the 1:1 whilst dashed lines represent  $\pm 1RSD$ .

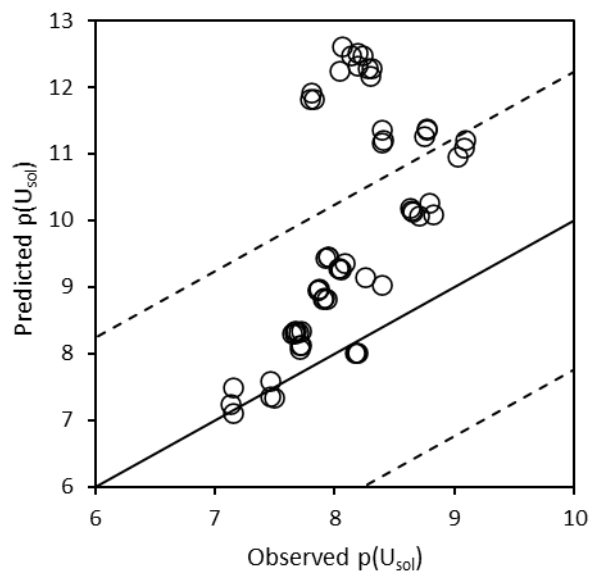


**Table S1.** Modelled kinetic parameters for  $U_{sol}$ .

	T1/2	A	B
	days	$\mu\text{g g}^{-1}$	$\mu\text{g g}^{-1}$
<b>BY-W</b>	49	30	25
<b>DY-M</b>	53	8	4
<b>PE-W</b>	57	18	25
<b>WK-W</b>	61	19	17
<b>IH-W</b>	56	14	15
<b>DY-G</b>	61	4	14
<b>BC-M</b>	70	18	11
<b>WK-A</b>	251	5	6
<b>TK-G</b>	46	7.7	4.84
<b>SB-G</b>	115	11	8
<b>EV-A</b>	73	1	1
<b>FD-G</b>	39	3	3
<b>CO-A</b>	181	6	7
<b>NP-A</b>	79	13	18
<b>SR-G</b>	65	29	14
<b>BH-G</b>	44	2	2
<b>BH-W</b>	31	4	3
<b>WS-A</b>	109	13	7
<b>SR-A</b>	124	53	96
<b>SR-W</b>	39	114	36

**Table S2.** Modelled kinetic parameters for  $U_E$ .

	T1/2	A	B
	days	$\mu\text{g g}^{-1}$	$\mu\text{g g}^{-1}$

<b>BC-M</b>	201	2194	2893
<b>DY-G</b>	204	2122	3108
<b>DY-M</b>	516	2130	2196
<b>IH-W</b>	66	2359	3811
<b>PE-W</b>	100	2775	3335
<b>WK-W</b>	376	2325	2611
<b>BY-W</b>	80	2399	3548
<b>CO-A</b>	136	2139	3170
<b>EV-A</b>	77	5312	2668
<b>FD-G</b>	24	3673	4103
<b>NP-A</b>	93	3037	2509
<b>SB-G</b>	466	3132	2381
<b>TK-G</b>	74	4223	3357
<b>WK-A</b>	368	1479	3289
<b>BH-G</b>	167	2755	3357
<b>BH-W</b>	348	2514	2298
<b>SR-A</b>	263	3662	1658
<b>SR-G</b>	92	1900	3669
<b>SR-W</b>	245	2231	2912
<b>WS-A</b>	33	3670	1743